Springer Proceedings in Physics 315

Asit Saha
Santo Banerjee *Editors*

Proceedings of the 2nd International Conference on Nonlinear Dynamics and Applications (ICNDA 2024), Volume 2

Complex Systems, Fractals and Nonlinear Flows

Springer

A Numerical Analysis of MHD Micropolar Hybrid Nanofluid Flow Over a Porous Stretching/Shrinking Sheet

Shiva Rao[1](✉) and P. N. Deka[2]

[1] Department of Mathematics, Bapujee College, Barpeta 781307, India
shivarao374@gmail.com
[2] Department of Mathematics, Dibrugarh University, Dibrugarh 786004, India
pndeka@dibru.ac.in

Abstract. This study investigates the behaviour of a two-dimensional, time-independent, and incompressible magnetohydrodynamic (MHD) flow of a hybrid nanofluid made of water and single-walled carbon nanotubes (SWCNT) and multi-walled carbon nanotubes (MWCNT). The research centers on analyzing a sheet undergoing stretching or shrinking within a porous medium subject to suction and a no-slip condition. It examines the influences of thermal radiation, heat generation, viscous dissipation, and Joule heating on the system. Through a suitable similarity transformation, nonlinear ordinary differential equations are derived from the governing equations, and the Keller-box numerical method is utilized to solve them. Our analysis includes graphical representations of the velocity profile, angular velocity profile, and temperature profile. Our findings indicate that the hybrid nanofluid consisting of SWCNTs and MWCNTs in water yields better results than other hybrid nanofluids, as well as single nanoparticle nanofluids. This study also offers a comprehensive comparison with previously published works. The research fills a gap in the current understanding of the behaviour of hybrid nanofluids in MHD flows, and has important implications for practical engineering problems.

Keywords: magnetohydrodynamics · thermal radiation · viscous dissipation · Joule heating · hybrid nanofluid · Stretching/shrinking sheet

1 Introduction

A nanofluid is a specialized fluid containing nanoparticles suspended within it, typically with sizes ranging from 1 to 100 nm. These nanoparticles are commonly crafted from materials like metals, metal oxides, and carbon-based compounds. Nanofluids present unique characteristics that make them an intriguing field for exploration in various engineering realms, spanning thermal management, energy conversion, and biomedical applications. Nanofluids offer a significant advantage over conventional fluids due to their enhanced heat transfer properties. By dispersing nanoparticles within the fluid, nanofluids effectively increase the surface area, leading to improved thermal conductivity. This

A. Saha and S. Banerjee (Eds.): ICNDA 2024, SPPHY 315, pp. 494–512, 2024.
https://doi.org/10.1007/978-3-031-69134-8_35

characteristic opens up various potential applications, such as utilizing nanofluids in electronic devices, heat exchangers, and cooling systems where efficient heat transfer is crucial. However, challenges persist, such as the need to address issues like nanoparticle agglomeration and the maintenance of stable suspensions.

Choi and Eastman's [7] pioneering work is often considered a seminal study in the nanofluids field. Their research demonstrated that incorporating small amounts of nanoparticles into a base fluid could significantly enhance its thermal conductivity. This discovery sparked considerable interest, prompting numerous subsequent investigations into nanofluid properties. For example, Lee *et al.* [27] conducted experiments to measure the thermal conductivity of fluids containing oxide nanoparticles. Utilizing a transient hot-wire method, they found that the nanofluids exhibited higher thermal conductivity than the base fluid. Later, Xuan and Li [60] observed that the thermal conductivity of nanofluids increased with higher nanoparticle concentration and smaller particle size, especially in fluids with higher thermal conductivity. Buongiorno [5] developed a theoretical model describing nanofluid transport behavior, revealing significant enhancements in thermal conductivity and viscosity compared to base fluids. Eastman *et al.* [13] explored nanofluid heat transfer properties in laminar flow, discovering a significantly higher heat transfer coefficient in nanofluids compared to the base fluid, with enhancement proportional to nanoparticle concentration. Kuznetsov and Nield [26] applied Buongiorno's model to analyze thermal conductivity's impact on the boundary layer stream and they found that the reduced Nusselt number decreases with the increase in Brownian motion parameter and thermophoresis parameter, while Khan and Pop [23] investigated steady nanofluid flow on a stretching sheet and discovered that Sherwood number is increasing for higher Prandtl number. Makinde and Aziz [32] explored nanofluid heat transfer characteristics under convective boundary conditions. Rao and Deka [43] conducted a computational study on the flow of Williamson nanofluid around a cylinder, revealing that thermal radiation significantly influences the nanofluid's heat transfer characteristics. Additionally, Das *et al.* [9] investigated the magnetohydrodynamic (MHD) mixed convection flow of aluminum-water nanofluid within a vertical duct, highlighting that both the Hartmann number and the Reynolds number play crucial roles in enhancing the fluid's heat transfer capabilities. Recent advancements by Hamzat *et al.* [16], Ma *et al.* [29], Mishra *et al.* [34], and Nabwey *et al.* [36] have further contributed to the evolving landscape of nanofluid research.

In the ongoing research on fluid flow over a stretching sheet, the investigation of fluid flow over a shrinking sheet has recently attracted significant interest. Miklavcic and Wang [33] were the first to analyze viscous flow over a shrinking sheet with suction applied at the boundary, paving the way for numerous subsequent studies on this subject. In contrast to the stretching sheet example, in this scenario, the sheet moves in the opposite direction, leading the flow towards a slot. Recent contributions include the numerical investigation by Swain *et al.* [54], who explored the impact of chemical reaction and magnetic fields on the flow of $MWCNT - Fe_2O_3/water$ hybrid nanofluid caused by an exponentially shrinking porous sheet under slip conditions.

Waini *et al.* [58] investigated how Joule heating, viscous dissipation, and thermal radiation influence the flow of an MHD micropolar hybrid nanofluid over a sheet undergoing stretching or shrinking. Recently, Rao and Deka [40] studied the heat transfer properties

of MHD Casson nanofluid over a porous stretching sheet and found that magnetic field and thermal radiation both enhances the heat transfer ability of the fluid. Vishalakshi *et al.* [56] conducted a study on non-Newtonian fluid flow over a porous stretching/shrinking sheet under the influence of mass transmission and thermal radiation. In the expansive realm of nanofluids, Rao and Deka [42] conducted detailed numerical investigations to explore the effects of solar radiation on heat and mass transfer phenomena. Similarly, many non-linear dynamical systems have been studied in the book edited by Banerjee and Saha [3]. Furthermore, Rao and Deka [39] extended their research to a numerical examination of MHD steady flow and its impact on chemical reactions and thermal radiation of Casson nanofluid over a stretching sheet. These studies collectively contribute to the evolving understanding of fluid dynamics over deformable surfaces and the various factors influencing the flow behavior.

Research on carbon nanofluids for diverse applications in nanotechnology and medicine has intensified since Iijima's [20] discovery of carbon nanotube (CNT) nanoparticles in 1991. CNTs, with their remarkable thermal and electrical properties, exhibit enhanced efficiency in a base fluid due to robust C-C bonds. Prajapati *et al.* [38] and Khalid *et al.* [22] note a 15 times higher thermal conductivity than copper and 1000 times greater capability in CNTs. Used in nanotechnology fields such as hardware, optics, and biomedicine, CNTs are categorized as single-walled (SWCNTs) or multi-walled (MWCNTs) based on graphite layers. Recent research by Kumaresan *et al.* [24] shows that low nanoparticle volume enhances heat transfer rates in CNT-containing nanofluids. Mahanthesh *et al.* [31] found SWCNT nanofluids exhibit a more even temperature distribution than MWCNT nanofluids. Ongoing advancements in CNT nanoparticle-based nanofluid research include studies by Alsagri *et al.* [2], Hossain *et al.* [18], Omri *et al.* [37], Sajid *et al.* [47], Rehman *et al.* [46], and Maatki *et al.* [30].

Hybrid nanofluids represent an innovative category of nanocomposite fluids, showing great promise across a range of industrial and engineering sectors due to their distinctive characteristics. These fluids are composed of a base fluid, like water or oil, infused with nanoparticles sourced from various materials, including metals, oxides, or carbon-based substances. The amalgamation of these elements leads to amplified thermal conductivity, increased heat transfer efficiency, and heightened stability compared to conventional fluids. Hybrid nanofluids are extensively employed in numerous applications such as heat exchange systems, cooling mechanisms, electronic equipment, and energy infrastructure. Their capacity to enhance thermal performance while maintaining compatibility with fluid systems renders them invaluable in optimizing the effectiveness and sustainability of diverse processes and technologies. As ongoing research reveals further insights into their capabilities, hybrid nanofluids are positioned to become instrumental in addressing the evolving challenges encountered in contemporary engineering and industry. Ongoing research aims to understand their properties and optimize performance, with studies like those by Suresh *et al.* [53], Sarkar *et al.* [48], Hayat and Nadeem [17], and Sundar *et al.* [52] contributing to this understanding. Rao and Deka [44] studied a MHD flow of hybrid nanofluid consist of SWCNT and Al_2O_3 nanoparticles past a permeable cone and found that hybrid nanofluid outperform ordinary nanofluid in many cases. Rao and Deka [41] also made an analysis of MHD flow of a hybrid nanofluid containing motile microorganism over a porous stretching sheet and found that microorganism stabilizes

the hybrid nanofluid flow. Recent advancements, including the work of Muneeshwaran *et al.* [35], Shoeibi *et al.* [50], Sheikholeslami [49], Kursus *et al.* [25], Dinarvand *et al.* [12], and Ullah *et al.* [55] further enrich the growing comprehension of hybrid nanofluids' capabilities and applications.

The study of non-Newtonian fluid flow is a topic of considerable academic research and practical importance, encompassing a wide range of substances such as volcanic lava, molten polymers, penetrating mud, oils, specific paints, liquid suspensions, food, cosmetics, and more, all with diverse mechanical applications. Various numerical models with distinct constitutive conditions and specific parameters have been proposed in the literature to capture the behavior of non-Newtonian fluids. The micropolar liquid model, in particular, finds application in understanding the flow characteristics of unusual oils, animal blood, fluid crystals with solid atoms, specific organic liquids, and solutions that are either colloidal or suspended in another medium. In micropolar liquids, pair tensions, spin inertia, and the microscopic motion of the liquid's components play significant roles. Hsiao [19] explored the heat and mass transfer behavior of MHD micropolar nanofluid near a stretching sheet, taking into account viscous dissipation. Dawar *et al.* [10] investigated two-dimensional electrically conducting and chemically reactive MHD micropolar flow over a stretching sheet with slip effect. Kausar *et al.* [21] studied how thermal radiation and viscous dissipation influence the flow of an MHD micropolar nanofluid approaching a permeable stretching sheet. Other authors have also contributed to the micropolar nanofluid models, as referenced in Almakki *et al.* [1], Dharmaiah *et al.* [11], Habib *et al.* [15], and Lone *et al.* [28].

The exploration of micropolar fluid dynamics has garnered growing attention owing to its wide-ranging applications across diverse industries. These include areas such as animal blood dynamics, solidification processes in liquid crystals, cooling of bath metal plates, handling of suspension and colloidal solutions, polymer fluid extrusion, and development of specialized lubricants. In this context, the present study investigates the MHD flow of micropolar hybrid nanofluid on a permeable stretching/shrinking sheet in the presence of thermal radiation under suction effect. The effects of viscous dissipation, Joule heating, and heat generation on the flow are also examined. To create the SWCNT/water nanofluid, SWCNT nanoparticles with a volume fraction ($\phi_1 = 0.1$) are first suspended in the base fluid. Subsequently, MWCNT nanoparticles with a volume fraction ($\phi_2 = 0.1$) are added to create the SWCNT-MWCNT/water hybrid nanofluid. The governing partial differential equations are transformed into ordinary differential equations using similarity transformation, and numerical solutions are obtained using the Keller-box method. The study also compares the performance of different hybrid nanoparticles with that of the SWCNT-MWCNT/water hybrid nanofluid.

2 Mathematical Formulations

Our investigation focuses on the flow of a steady two-dimensional laminar and incompressible micropolar hybrid nanofluid that contains two types of nanoparticles (single-walled carbon nanotubes [SWCNT] and multi-walled carbon nanotubes [MWCNT]) over a permeable sheet that can stretch or shrink. This nanofluid is water-based and electrically conducting. We have tabulated the thermophysical properties of the nanofluid in

Table 1, while the thermophysical properties model for the hybrid nanofluid is specified in Table 2.

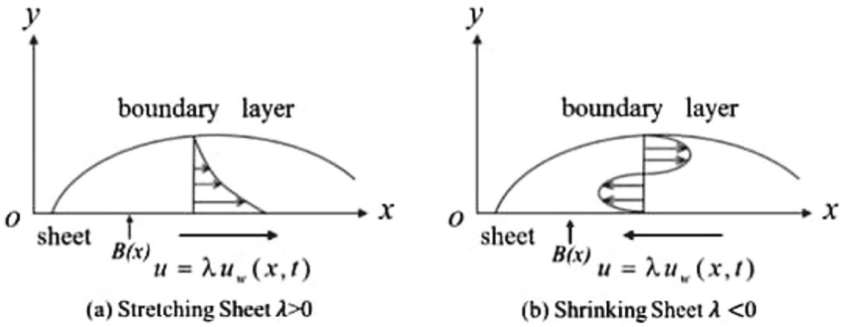

Fig. 1. Schematic diagram of the problem

The velocity of a stretching or shrinking sheet can be expressed as $u_w(x) = \lambda ax$, where λ is a constant. A positive λ value corresponds to a stretching sheet, while a negative λ value corresponds to a shrinking sheet.

The velocity of mass transfer at the boundary can be denoted as $v_w(x) = v_o$, where a negative v_o value signifies suction. The x-axis measures distance along the stretching surface in the direction of movement, while the y-axis lies perpendicular to it. A uniform magnetic field with magnitude B is applied parallel to the y-axis. We postulate that the magnetic field is represented as $B = (0,0, B_o)$, and the induced magnetic field due to fluid motion is deemed insignificant compared to the applied field. This assumption is substantiated by the low magnetic Reynolds number observed in metallic liquids and partially ionized fluids [8]. Furthermore, we assume the absence of an external electric field, hence the negligible impact of fluid polarization. The physical model is illustrated in Fig. 1.

Table 1. Thermophysical properties of nanoparticles and water

	$\rho(kg/m^3)$	$\kappa(W/mK)$	$\sigma(s/m)$	$C_p(J/kgK)$
SWCNT	2600	6600	1×10^6	425
MWCNT	1600	3000	1×10^7	796
H_20	997.1	0.613	5.5×10^{-6}	4179

The governing equation of the flow along with boundary conditions are given below [23, 58]:

$$\frac{\partial u}{\partial x} + \frac{\partial v}{\partial y} = 0 \tag{1}$$

$$\rho_{hnf}\left(u\frac{\partial u}{\partial x} + v\frac{\partial u}{\partial y}\right) = \left(\mu_{hnf} + k_1\right)\frac{\partial^2 u}{\partial y^2} + k_1\frac{\partial N}{\partial y} - \sigma_{hnf}B_o^2 u - \mu_{hnf}\frac{u}{k_o}, \tag{2}$$

$$j\rho_{hnf}\left(u\frac{\partial N}{\partial x}+v\frac{\partial N}{\partial y}\right)=\gamma_{hnf}\frac{\partial^2 N}{\partial y^2}-k_1\left(2N+\frac{\partial u}{\partial y}\right), \tag{3}$$

$$u\frac{\partial T}{\partial x}+v\frac{\partial T}{\partial y}=\frac{\kappa_{hnf}}{\left(\rho C_p\right)_{hnf}}\frac{\partial^2 T}{\partial y^2}+\frac{\mu_{hnf}}{\left(\rho C_p\right)_{hnf}}\left(\frac{\partial u}{\partial y}\right)^2+\frac{\sigma_{hnf}}{\left(\rho C_p\right)_{hnf}}B_o^2u^2 + \frac{Q_o}{\left(\rho C_p\right)_{hnf}}(T-T_\infty)-\frac{1}{\left(\rho C_p\right)_{hnf}}\frac{\partial q_r}{\partial y} \tag{4}$$

Initial and boundary conditions are outlined below:

$$u=u_w=\lambda ax, v=v_w=v_o, N=-m_o\frac{\partial u}{\partial y}T=T_w \quad when\ y=0$$
$$u\to 0 \quad N\to 0 \quad T\to 0 \quad as \quad y\to\infty \tag{5}$$

The mathematical expression for the Rosseland approximation of radiative heat flux, as detailed by Sparrow [51], Brewster [4], and Raptis [45], is as follows:

$$\frac{\partial q_r}{\partial y}=\frac{-4\sigma^*}{3k^*}\frac{\partial T^4}{\partial y}, \tag{6}$$

We can obtain the following expression by extending the Taylor series and neglecting the higher-order terms:

$$T^4=4T_\infty^3T-3T_\infty^4,$$

Hence Eq. (6) becomes-

$$\frac{\partial q_r}{\partial y}=\frac{-16\sigma^*}{3k^*}T_\infty^3\frac{\partial^2 T}{\partial y^2}, \tag{7}$$

The similarity transformation are used as follows [58]-

$$\eta=\sqrt{\frac{a}{v_f}}y,\ \psi=\sqrt{av_f}xf(\eta), N=ax\sqrt{\frac{a}{v_f}}G(\eta),$$
$$\theta(\eta)=\frac{T-T_\infty}{T_w-T_\infty}, u=\frac{\partial\psi}{\partial y}=axf\prime(\eta), v=-\frac{\partial\psi}{\partial x}=-\sqrt{av_f}f(\eta) \tag{8}$$

Substituting Eq. (8) in the governing Eq. (1) to (4) we get:

$$(A_1+K)f'''+A_2ff''-A_2f'2+KG'-(A_5M+A_1K_p)f'=0, \tag{9}$$

$$\left(A_1+\frac{K}{2}\right)G''+A_2G'f-A_2Gf'-K\left(2G+f''\right)=0, \tag{10}$$

$$\frac{\theta''}{Pr}(A_4+Rd)+A_3f\theta'+A_1Ecf''^2+A_5MEcf'^2+Q\theta=0, \tag{11}$$

Table 2. Hybrid nanofluid's Thermophysical properties model [58]

Property	*Hybridnanofluid*
Density	$\rho_{hnf} = (1-\phi_2)\left[(1-\phi_1)\rho_f + \phi_1\rho_{s1}\right] + \phi_2\rho_{s2}$
Dynamic viscosity	$\mu_{hnf} = \frac{\mu_f}{(1-\phi_1)^{2.5}(1-\phi_2)^{2.5}}$
Heat Capacity	$(\rho C_p)_{hnf} = (1-\phi_2)\left[(1-\phi_1)(\rho C_p)_f + \phi_1(\rho C_p)_{s1}\right] + \phi_2(\rho C_p)_{s2}$
Thermal Conductivity	$\kappa_{hnf} = \frac{\kappa_{s2}+2\kappa_{nf}-2\phi_2(\kappa_{nf}-\kappa_{s2})}{\kappa_{s2}+2\kappa_{nf}+\phi_2(\kappa_{nf}-\kappa_{s2})} \times \kappa_{nf}$ $where, \kappa_{nf} = \frac{\kappa_{s1}+2\kappa_f-2\phi_1(\kappa_f-\kappa_{s1})}{\kappa_{s1}+2\kappa_f+\phi_1(\kappa_f-\kappa_{s1})} \times \kappa_f$
Electrical conductivity	$\sigma_{hnf} = \left[1 + \frac{3\left(\frac{\sigma_{s2}}{\sigma_{nf}}-1\right)\phi_2}{\left(\frac{\sigma_{s2}}{\sigma_{nf}}+2\right)-\left(\frac{\sigma_{s2}}{\sigma_{nf}}-1\right)\phi_2}\right] \times \sigma_{nf}$ $where, \sigma_{nf} = \left[1 + \frac{3\left(\frac{\sigma_{s1}}{\sigma_f}-1\right)\phi_1}{\left(\frac{\sigma_{s1}}{\sigma_f}+2\right)-\left(\frac{\sigma_{s1}}{\sigma_f}-1\right)\phi_1}\right] \times \sigma_f$

By applying the similarity transformation, we can rewrite boundary condition of Eq. (5) as:

$$f(0) = S \quad f'(0) = \lambda \quad g(0) = -m_o f''(0) \quad \theta(0) = 1$$

$$f'(\infty) \to 0 \quad g(\infty) \to 0 \quad \theta(\infty) \to 0 \tag{12}$$

By the following definitions, we can establish the values of $A_i (i = 1, 2, 3, 4, 5)$:

$$A_1 = \frac{\mu_{hnf}}{\mu_f}, A_2 = \frac{\rho_{hnf}}{\rho_f}, A_3 = \frac{(\rho C_p)_{hnf}}{(\rho C_p)_f}, A_4 = \frac{\kappa_{hnf}}{\kappa_f}, A_5 = \frac{\sigma_{hnf}}{\sigma_f},$$

The following specification is made for the flow parameters:

$$M = \frac{\sigma_f B_o^2}{a\rho_f}, K_p = \frac{\nu_f}{ak_o}, K = \frac{k_1}{\mu_f}, \gamma_{hnf} = \left(\mu_{hnf} + \frac{k_1}{2}\right)j, Pr = \frac{\nu_f(\rho C_p)_f}{\kappa_f},$$
$$Rd = \frac{16\sigma^* T_\infty^3}{3k^*\kappa_f}, Ec = \frac{(ax)^2\rho_f}{(\rho C_p)_f(T_w - T_\infty)}, Q = \frac{Q_o}{a(\rho C_p)_f}, j = \frac{\nu_f}{a}$$

The study focuses on various physical quantities that play a crucial role in a wide range of engineering applications and industrial processes. The physical parameters are defined as follows:

$$Cf_x = \frac{1}{\rho_f u_w^2}\left[(\mu + k_1)\left(\frac{\partial u}{\partial y}\right)_{y=0} + k_1(N)_{y=0}\right],$$

$$Cn_x = \frac{x}{a}\left(\frac{\partial N}{\partial y}\right)_{y=0}, Nu_x = -\frac{x\kappa_{hnf}}{\kappa_f(T_w - T_\infty)}\left(\frac{\partial T}{\partial y}\right)_{y=0} \tag{13}$$

From Eq. (8) and (13) we get:

$$Re_x^{\frac{1}{2}} Cf_x = (1 + (1-n)K)f''(0),$$

$$Re_x^{-1} C_n = G'(0)$$

$$Re_x^{-\frac{1}{2}} Nu_x = -\frac{\kappa_{hnf}}{\kappa_f}\theta'(0)$$

where, the local Reynolds number, $Re_x = \frac{xu_w}{\nu_f}$

3 Method of Solution

The Keller-box technique emerges as a robust numerical approach employed to solve a non-linear system of equations describing, specifically Eq. (9) to (11) accompanied by boundary condition (12). This method is selected for its adaptability and notable precision, showcasing an error order of 10^{-5} in resolving analogous problems. Its implementation in this context follows the technique established by Cebeci and Bradshaw [6].

The algorithm within the Keller-box technique unfolds through several key steps. Initially, the derived ODEs undergo conversion into a system of 1st order equations, a pivotal step aimed at simplifying the solution process and rendering the problem amenable to finite difference equations. Subsequently, these reduced equations are transformed into finite difference equations. The next phase involves the linearization of these equations utilizing the Newton method, expressing them in vector form. This linearization, a crucial step, entails approximating non-linear terms with linear functions. The resulting system of linear equations is then solvable using a tri-diagonal matrix. This meticulous process facilitates the iterative solution of the linearized equations, thanks to the widely employed Newton method renowned for addressing non-linear problems. By following these computational procedures, the Keller-box method skillfully furnishes a numerical resolution to the initial non-linear issue with outstanding precision.

4 Results and Discussion

To explore the physical manifestation of the issue, we've showcased numerical outcomes using both visual representations and tabulated formats. Velocity and temperature profiles have been depicted graphically to illustrate the influence of various factors. Employing MATLAB code, we've executed the Keller-box approach to produce these graphs and associated numerical data. Our findings have been juxtaposed with previously documented results from studies by Wang *et al.* (1989), Khan and Pop (2010), and Waini *et al.* (2019) to corroborate our conclusions. Table 3 demonstrates strong adherence and enhanced precision, instilling confidence in the effectiveness of our methodology and the robustness of our analysis.

Table 3. Comparison for values of $-\theta'(0)$ for ordinary fluid ($\phi_1 = 0 and \phi_2 = 0$) with various values of Pr when $K = M = K_p = Rd = E_c = Q = 0$ and $\lambda = 1$.

Pr	*KhanandPop* [23]	*Wangetal.*[59]	*Wainietal.* [57]	*Present*
2	0.9113	0.9114	0.911353	0.9114
6.13	–	–	1.759682	1.7597
7	1.8954	1.8954	1.895400	1.8954
20	3.3539	3.3539	3.353902	3.3540

Table 4. Comparison for the values of $C_n Re_x^{-1}$ for $Cu/water$ nanofluid for different values of S when $K = Pr = M = K_p = Rd = E_c = Q = 0$.

S	$C_n Re_x^{-1}$					
	$\phi = 0.05$		$\phi = 0.1$		$\phi = 0.2$	
	Gangadhar *et al.* [14]	Present	Gangadhar *et al.* [14]	Present	Gangadhar *et al.* [14]	Present
0	−0.268876	−0.2651	−0.282042	−0.2818	−0.290563	−0.2910
1	−0.551181	−0.5509	−0.587866	−0.5734	−0.612038	−0.6098
2	−1.047061	−1.0501	−1.130075	−1.1245	−1.185313	−1.1845
2.5	−1.389396	−1.3675	−1.505597	−1.3576	−1.583130	−1.5820
3	−1.798858	−1.7910	−1.955260	−1.9479	−2.059818	−2.0593

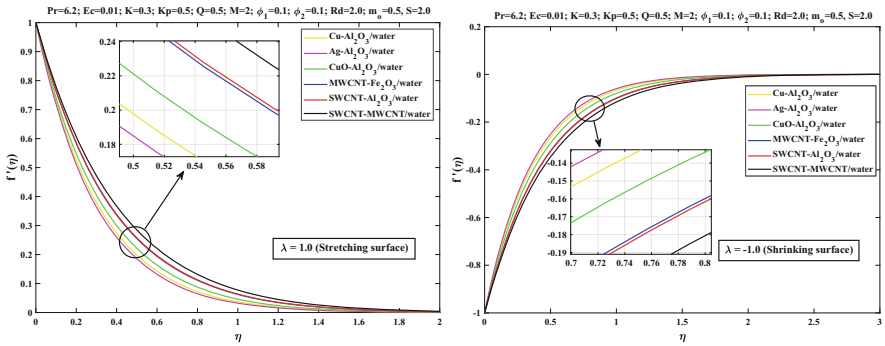

Fig. 2. Velocity distribution's comparison of different hybrid nanofluids for both surfaces

Table 4 intends to draw a comparison of our results with that of Gangadhar *et al.* for the values of $C_n Re_x^{-1}$ for $Cu - Al_2O_3/water$ hybrid nanofluid for different values of S.

Figure 2, 3 and 4 exhibits the velocity, angular velocity and temperature distribution for both stretching and shrinking surface in the presence of various types of hybrid nanoparticles such as $Cu - Al_2O_3, Ag - Al_2O_3, CuO - Al_2O_3, MWCNT - Fe_2O_3, SWCNT - Al_2O_3$ and $SWCNT - MWCNT$ in the base fluid (water) for $\phi_1 = \phi_2 = 0.1$. When a sheet is stretched, the $Ag - Al_2O_3$/water hybrid nanofluid displays a slower velocity and angular velocity profile, while the $SWCNT - MWCNT$/water hybrid nanofluid shows the highest velocity and angular velocity profile among other hybrid nanoparticles. Conversely, when the sheet shrinks, the trends are reversed for both velocity and angular velocity profiles. Additionally, it's noted that for both stretching and shrinking surfaces, the $SWCNT - MWCNT$/water hybrid nanofluid exhibits the highest temperature profile compared to other hybrid nanofluids.

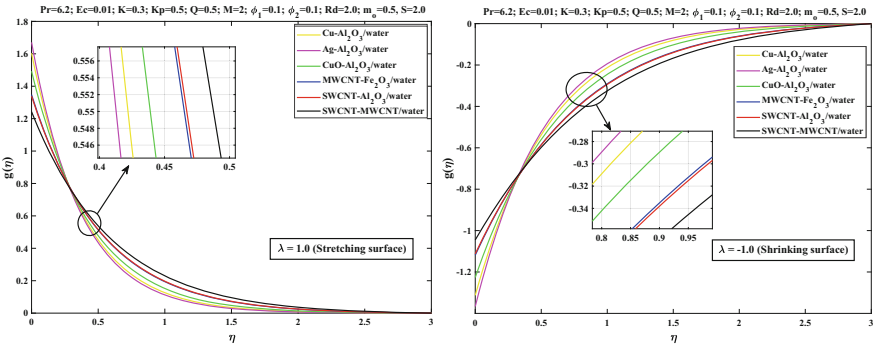

Fig. 3. Angular velocity distribution's comparison of different hybrid nanofluids for both surfaces

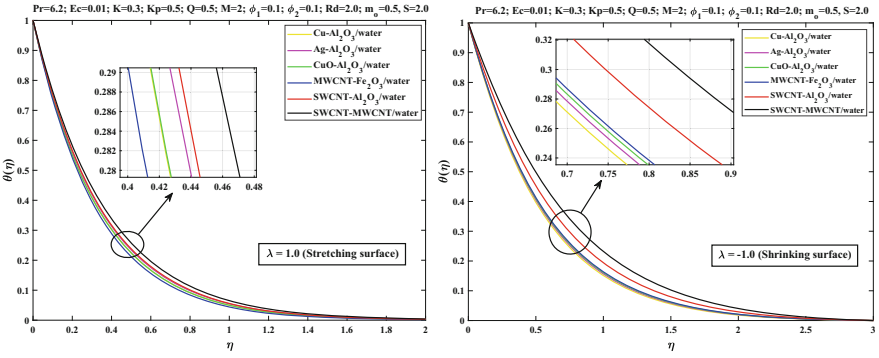

Fig. 4. Temperature distribution's comparison of different hybrid nanofluids for both surfaces

Figures 5, 6 and 7 represent the influence of magnetic parameter of the $SWCNT - MWCNT/water$ hybrid nanofluid as well as $SWCNT/water$ nanofluid on velocity, angular velocity and temperature profile. The flow velocity of the hybrid nanofluid decreases, while the angular velocity and temperature profile increase with higher values of M on

the stretching surface. Conversely, the results are opposite for the shrinking surface compared to the stretching surface. It is observed that the velocity profile increases whereas the angular velocity and temperature profile falls with the increase in the value of M. Additionally, it is also observed that the $SWCNT - MWCNT/water$ hybrid nanofluid outperforms the $SWCNT/water$ nanofluid interms of all the three profiles.

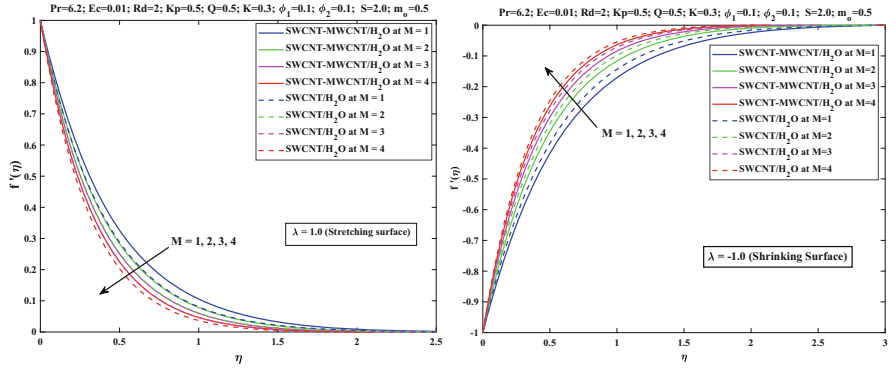

Fig. 5. Velocity profile of M for both surfaces

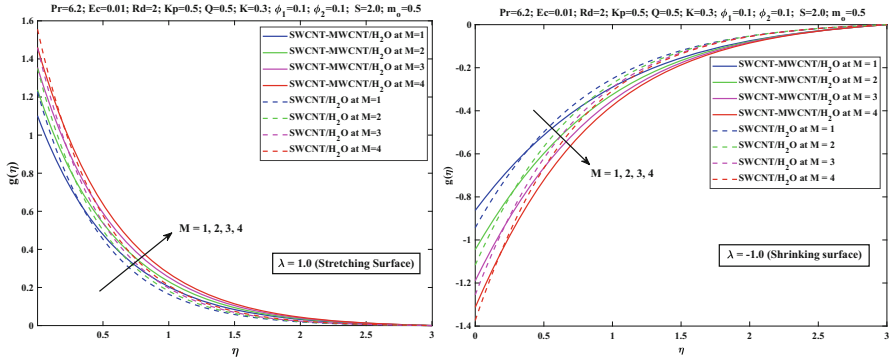

Fig. 6. Angular velocity profile of M for both surfaces

The influences of material parameter K for both the hybrid nanofluid ($SWCNT - MWCNT$) as well the nanofluid with single nanoparticles ($SWCNT$) on the velocity, angular velocity and temperature profile for both stretching and shrinking surface are presented in Fig. 8, 9 and 10. Figure 8 illustrates the velocity profile for both stretching and shrinking surfaces across different values of K. It's evident that the velocity profile increases for the stretching sheet but decreases for the shrinking surface. Figure 9 and 10 reveal that both the angular velocity profile and temperature profile decrease with increasing values of K for the stretching sheet, while for the shrinking sheet, these profiles increase with K. It's apparent from the figures that the performance of the hybrid nanofluid surpasses that of nanofluids containing single nanoparticles for material parameters as well.

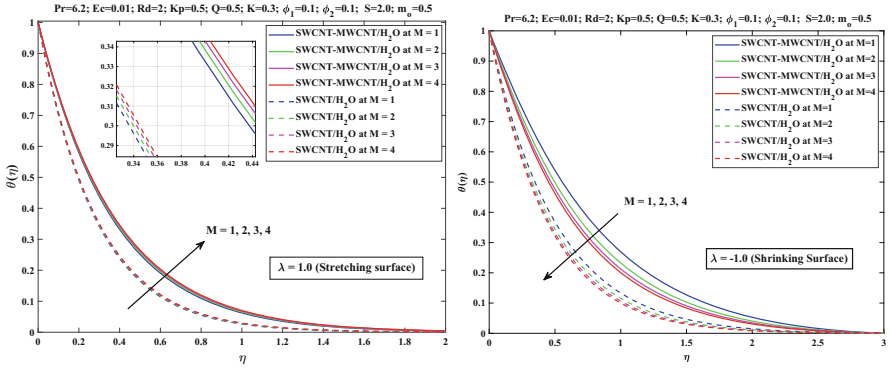

Fig. 7. Temperature profile of M for both surfaces

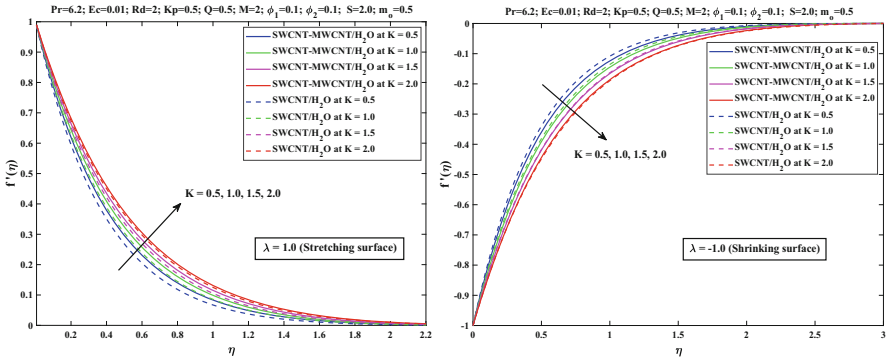

Fig. 8. Velocity profile of K for both surfaces

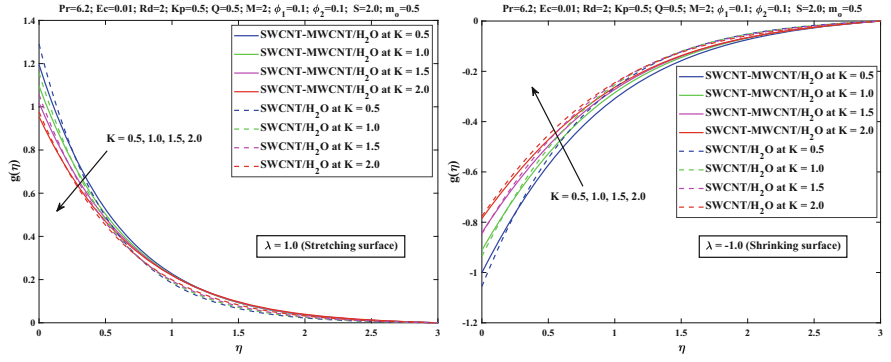

Fig. 9. Angular velocity profile of K for both surfaces

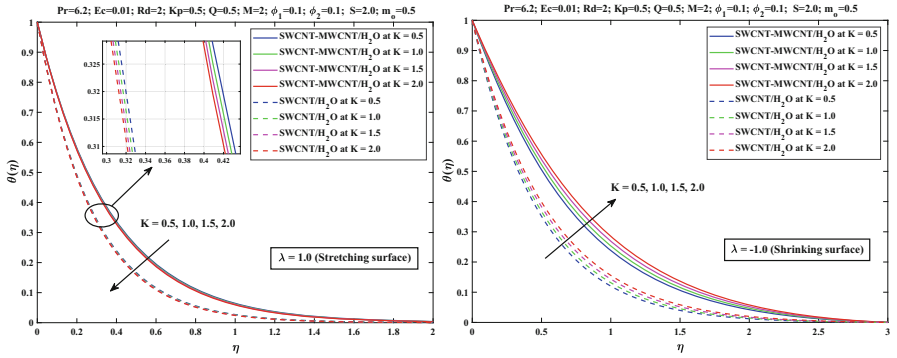

Fig. 10. Temperature profile of K for both surfaces

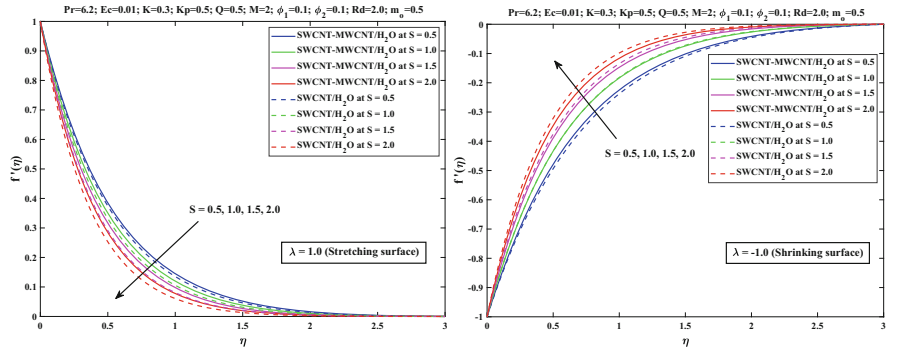

Fig. 11. Velocity profile of S for both surfaces

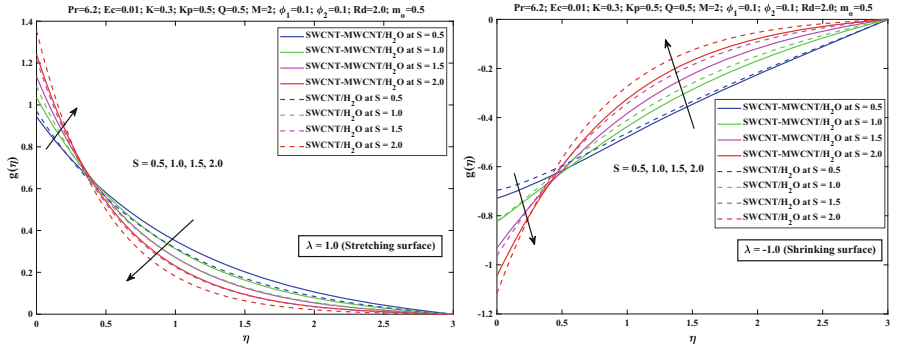

Fig. 12. Angular velocity profile of S for both surfaces

Figure 11 depicts the influence of suction effect (S) on the flow of both $SWCNT-MWCNT/water$ hybrid nanofluid as well as $SWCNT/water$ nanofluid for the case of both stretching and shrinking surface. It is found that in the case of stretching surface the velocity profile decreases with the increase in the value of S whereas the velocity profile

increases as we go on increasing the value of suction parameter. Figure 12 presents the graphical representation of the angular velocity curve for different suction parameter (S) values. It's noted that for the stretching surface, the angular velocity profile initially increases and then decreases with the rising suction parameter value. Conversely, for the shrinking sheet, the angular velocity profile exhibits an opposite trend, starting with an initial rise and then declining as the suction parameter increases.

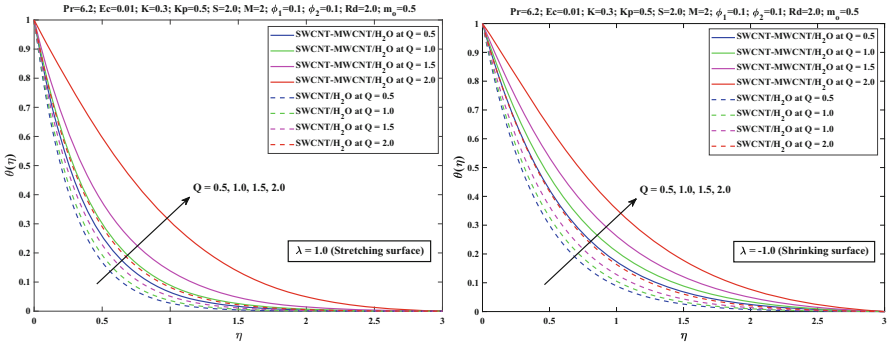

Fig. 13. Temperature profile of Q for both surfaces

Figure 13 illustrates the performance comparison between the hybrid nanofluid ($SWCNT - MWCNT$) and the conventional nanofluid ($SWCNT$) regarding the temperature profile under various heat generation/absorption (Q) values for both stretching and shrinking surfaces. It's evident from the figure that the temperature rises as the value of Q increases in both cases.

5 Conclusion

In this study, we explore the efficiency of heat transfer in a hybrid nanofluid flow under the combined influence of magnetohydrodynamics (MHD) and micropolar effects, alongside porous stretching or shrinking sheets in a two-dimensional steady state, with suction effects taken into account. Employing the Keller Box Scheme for numerical analysis due to its demonstrated accuracy in parabolic problem computation, we find that using a hybrid nanofluid yields superior performance compared to a single nanoparticle type nanofluid. Specifically, the $SWCNT - MWCNT$/water hybrid nanofluid outperforms other hybrids like $Cu - Al_2O_3$, $Ag - Al_2O_3$, $CuO - Al_2O_3$, $MWCNT - Fe_2O_3$, and $SWCNT - Al_2O_3$. For the stretching surface scenario, increasing magnetic field and suction effect reduces the flow velocity in the boundary layer, while elevated material parameter values increase the flow velocity. Angular velocity increases with stronger magnetic field effects but decreases with higher material parameters. Additionally, higher magnetic field and heat generation lead to increased temperature in the boundary layer, whereas higher material parameter values cause temperature decline. In contrast, for the shrinking surface case, velocity near the sheet increases under high magnetic field and suction, but

decreases with higher material parameters. The angular velocity increases with material parameter values but decreases with stronger magnetic fields. Moreover, increasing material parameter values and heat generation increase boundary layer temperature, while magnetic parameter increases lead to temperature profile depletion.

Abbreviations

Nomenclature

a Constant
B_o Magnetic field (T)
C Nanoparticle concentration (mol L^{-1})
Cf_x Skin-friction coefficient
Cn_x Couple stress
C_p Specific heat at constant pressure (J kg^{-1} K^{-1})
G Dimensional angular velocity
Ec Eckert number
j Microinertia per unit mass (kgm^{-1}))
K Micropolar/Material parameter
K_p Permeability parameter
Nu_x Nusselt number
k^* Mean absorption co-efficient (m^{-1})
k_o Porous term (m^2)
k_1 Vortex viscosity (m^2s^{-1})
N Microrotation or angular velocity whose direction is normal to XY-plane ($rads^{-1}$)
M Magnetic parameter
m_o Boundary parameter
Pr Prandtl number
Q_o Coefficient of heat generation (Wm^{-3})
q_r Radiative heat flux (Wm^{-2})
Rd Radiation parameter
Re_x Reynold number
T Temperature (K)
Q Heat generation/absorption
u, v Velocity component along x-axis and y-axis respectively (m s^{-1})
x, y Cartesian coordinates on the surface and perpendicular to it, respectively (m)

Greek Symbols:

ψ Stream function
ν Kinematic viscosity (m^2 s^{-1})
μ Dynamic viscosity (kg m^{-1} s^{-1})
σ Electrically conductivity (S m^{-1})
$f\prime$ Dimensionless velocity
κ Thermal conductivity of the nanofluid ($Wm^{-1}K^{-1}$)
γ Spin gradient viscosity ($kgm^{-1}s^{-1}$)

σ^* Stefan-Boltzmann coefficient ($Wm^{-2}K^{-4}$)
ϕ_1 Volume fraction of *SWCNT* nanoparticle
θ Dimensional temperature
ρ Density (kg m^{-3})
ϕ_2 Volume fraction of *MWCNT* nanoparticle
η Similarity variable

Superscript

$'$ Derivative w.r.t. η

***Subscript*:**

nf Single nanoparticles nanofluid
∞ Free stream region
hnf Hybrid nanofluid
*s*1 *SWCNT* Nanoparticle
f Base fluid
w Wall
*s*2 *MWCNT* Nanoparticle

References

1. M. Almakki, H. Mondal, P. Sibanda, Onset of unsteady MHD micropolar nanofluid flow with entropy generation. Int. J. Ambient Energy **43**(1), 4356–4369 (2021)
2. A. Alsagri et al., MHD thin film flow and thermal analysis of blood with CNTs nanofluid. Coatings **9**(3), 175 (2019)
3. Banerjee, S., Saha, A.: Nonlinear Dynamics and Applications. Springer Nature (2022).
4. Q.M. Brewster, Thermal Radiative Transfer and Properties, Solutions Manual (1st ed.). Wiley-Interscience (1992)
5. J. Buongiorno, Convective transport in nanofluids. J. Heat Transfer **128**(3), 240–250 (2005)
6. T. Cebeci, P. Bradshaw, Physical and Computational Aspects of Convective Heat Transfer. Physical and Computational Aspects of Convective Heat Transfer (1988)
7. S. U. S. Choi, J. Eastman, Enhancing thermal conductivity of fluids with nanoparticles. Argonne National Lab (United States) 66 (1995)
8. K.R. Cramer, S.I. Pai, *Magnetofluid Dynamics for Engineers and Applied Physicists* (McGraw-Hill, New York, 1973)
9. B.R. Das, P. Deka, S. Rao, Numerical analysis on MHD mixed convection flow of Al_2O_3/H_2O (Aluminum-Water) nanofluids in a vertical square duct. East Eur. J. Phys. **2**, 51–62 (2023)
10. A. Dawar, et al., Chemically reactive MHD micropolar nanofluid flow with velocity slips and variable heat source/sink. Scientific Reports **10**(1) (2020).
11. G. Dharmaiah, O.D. Makinde, K.S. Balamurugan, Influence of Magneto Hydro Dynamics (MHD) nonlinear radiation on Micropolar Nanofluid flow over a stretching surface: revised Buongiorno's Nanofluid model. J. Nanofluids **11**(6), 1009–1022 (2022)

12. S. Dinarvand, H. Berrehal, I. Pop, A.J. Chamkha, Blood-based hybrid nanofluid flow through converging/diverging channel with multiple slips effect: a development of Jeffery-Hamel problem. Int. J. Numer. Meth. Heat Fluid Flow **33**(3), 1144–1160 (2022)
13. J.A. Eastman, S.R. Phillpot, S.U.S. Choi, P. Keblinski, Thermal transport in Nanofluids. Annu. Rev. Mater. Res. **32**(1), 219–246 (2004)
14. K. Gangadhar, T. Kannan, P. Jayalakshmi, Magnetohydrodynamic micropolar nanofluid past a permeable stretching/shrinking sheet with Newtonian heating. J. Braz. Soc. Mech. Sci. Eng. **39**(11), 4379–4391 (2017)
15. Habib, D., Salamat, N., Ahsan, M., Abdal, S., Siddique, I., Ali, B.: Significance of bioconvection and mass transpiration for MHD micropolar Maxwell nanofluid flow over an extending sheet. Waves in Random and Complex Media, 1–15 (2022)
16. A.K. Hamzat, M.I. Omisanya, A.Z. Sahin, O. Ropo Oyetunji, N. Abolade Olaitan, Application of nanofluid in solar energy harvesting devices: a comprehensive review. Energy Convers. Manage. **266**, 115790 (2022)
17. T. Hayat, S. Nadeem, Heat transfer enhancement with Ag–CuO/water hybrid nanofluid. Results Phys. **7**, 2317–2324 (2017)
18. R. Hossain, A. Azad, M. Jahid Hasan, M. Rahman, Thermophysical properties of Kerosene oil-based CNT nanofluid on unsteady mixed convection with MHD and radiative heat flux. Eng. Sci. Technol. Int. J. **35**, 101095 (2022)
19. K.L. Hsiao, Micropolar nanofluid flow with MHD and viscous dissipation effects towards a stretching sheet with multimedia feature. Int. J. Heat Mass Transf. **112**, 983–990 (2017)
20. S. Iijima, Helical microtubules of graphitic carbon. Nature **354**(6348), 56–58 (1991)
21. M.S. Kausar, A. Hussanan, M. Waqas, M. Mamat, Boundary layer flow of micropolar nanofluid towards a permeable stretching sheet in the presence of porous medium with thermal radiation and viscous dissipation. Chin. J. Phys. **78**, 435–452 (2022)
22. A. Khalid, I. Khan, A. Khan, S. Shafie, I. Tlili, Case study of MHD blood flow in a porous medium with CNTS and thermal analysis. Case Stud. Thermal Eng. **12**, 374–380 (2018)
23. W. Khan, I. Pop, Boundary-layer flow of a nanofluid past a stretching sheet. Int. J. Heat Mass Transf. **53**(11–12), 2477–2483 (2010)
24. V. Kumaresan, R. Velraj, S.K. Das, Convective heat transfer characteristics of secondary refrigerant-based CNT nanofluids in a tubular heat exchanger. Int. J. Refrig **35**(8), 2287–2296 (2012)
25. M. Kursus, P.J. Liew, N.A. Che Sidik, J. Wang, Recent progress on the application of nanofluids and hybrid nanofluids in machining: a comprehensive review. Int. J. Adv. Manuf. Technol. **121**(3–4), 1455–1481 (2022)
26. A. Kuznetsov, D. Nield, Natural convective boundary-layer flow of a nanofluid past a vertical plate. Int. J. Therm. Sci. **49**(2), 243–247 (2010)
27. S. Lee, S.U.S. Choi, S. Li, J.A. Eastman, Measuring thermal conductivity of fluids containing oxide nanoparticles. J. Heat Transfer **121**(2), 280–289 (1999)
28. S.A. Lone, M.A. Alyami, A. Saeed, A. Dawar, P. Kumam, W. Kumam, MHD micropolar hybrid nanofluid flow over a flat surface subject to mixed convection and thermal radiation. Sci. Rep. **12**(1), 17283 (2022)
29. H. Ma, B. He, L. Su, D. He, Heat transfer enhancement of nanofluid flow at the entry region of microtubes. Int. J. Therm. Sci. **184**, 107944 (2023)
30. C. Maatki, Heat transfer enhancement using CNT-water nanofluids and two stages of seawater supply in the triangular solar still. Case Stud. Thermal Eng. **30**, 101753 (2022)
31. B. Mahanthesh, B. Gireesha, N. Shashikumar, S. Shehzad, Marangoni convective MHD flow of SWCNT and MWCNT nanoliquids due to a disk with solar radiation and irregular heat source. Physica E **94**, 25–30 (2017)
32. O. Makinde, A. Aziz, Boundary layer flow of a nanofluid past a stretching sheet with a convective boundary condition. Int. J. Therm. Sci. **50**(7), 1326–1332 (2011)

33. M. Miklavčič, C.Y. Wang, Viscous flow due to a shrinking sheet. Quart. Appl. Math. **64**(2), 283–290 (2006)
34. A. Mishra, A.K. Pandey, M. Kumar, Velocity, thermal and concentration slip effects on mhd silver–water nanofluid flow past a permeable cone with suction/injection and viscous-ohmic dissipation. Heat Transfer Research **50**(14), 1351–1367 (2019)
35. M. Muneeshwaran, G. Srinivasan, P. Muthukumar, C.C. Wang, Role of hybrid-nanofluid in heat transfer enhancement – a review. Int. Commun. Heat Mass Transfer **125**, 105341 (2021)
36. H.A. Nabwey, T. Armaghani, B. Azizimehr, A.M. Rashad, A.J. Chamkha, A comprehensive review of nanofluid heat transfer in porous media. Nanomaterials **13**(5), 937 (2023)
37. M. Omri, H. Smaoui, L. Frechette, L. Kolsi, A new microchannel heat exchanger configuration using CNT-nanofluid and allowing uniform temperature on the active wall. Case Stud. Thermal Eng. **32**, 101866 (2022)
38. V. Prajapati, P.K. Sharma, A. Banik, Carbon nanotubes and its applications. Int. J. Pharm. Sci. Res. **2**(5), 1099–1107 (2011)
39. S. Rao, P. Deka, A numerical solution using EFDM for unsteady MHD radiative Casson nanofluid flow over a porous stretching sheet with stability analysis. Heat Transfer **51**(8), 8020–8042 (2022)
40. S. Rao, P. Deka, A numerical study on heat transfer for mhd flow of radiative casson nanofluid over a porous stretching sheet. Latin Am. Appl. Res. Int. J. **53**(2), 129–136 (2023)
41. S. Rao, P. Deka, Analysis of MHD bioconvection flow of a hybrid nanofluid containing motile microorganisms over a porous stretching sheet. BioNanoScience **13**, 2134–2150 (2023)
42. S. Rao, P.N. Deka, A numerical investigation on transport phenomena in a nanofluid under the transverse magnetic field over a stretching plate associated with solar radiation, in *Nonlinear Dynamics and Applications. Springer Proceedings in Complexity*. ed. by S. Banerjee, A. Saha (Springer, Cham, 2022)
43. S. Rao, P.N. Deka, A numerical study on unsteady MHD williamson nanofluid flow past a permeable moving cylinder in the presence of thermal radiation and chemical reaction. Biointerface Res. Appl. Chem. **13**(5), 436 (2023)
44. Rao, S., Deka, P.N.: A study on MHD flow of SWCNT-Al2O3/water hybrid nanofluid past a vertical permeable cone under the influence of thermal radiation and chemical reactions. Numer. Heat Transfer, Part A: Appl. 1–21 (2023).
45. A. Raptis, Radiation and free convection flow through a porous medium. Int. Commun. Heat Mass Transfer **25**(2), 289–295 (1998)
46. A. Rehman, A. Saeed, Z. Salleh, R. Jan, P. Kumam, Analytical investigation of the time-dependent stagnation point flow of a CNT nanofluid over a stretching surface. Nanomaterials **12**(7), 1108 (2022)
47. M.U. Sajid, Y. Bicer, Impacts of ultrasonication time and surfactants on stability and optical properties of CuO, Fe3O4, and CNTs/water nanofluids for spectrum selective applications. Ultrason. Sonochem. **88**, 106079 (2022)
48. J. Sarkar, P. Ghosh, A. Adil, A review on hybrid nanofluids: Recent research, development and applications. Renew. Sustain. Energy Rev. **43**, 164–177 (2015)
49. M. Sheikholeslami, Numerical investigation of solar system equipped with innovative turbulator and hybrid nanofluid. Sol. Energy Mater. Sol. Cells **243**, 111786 (2022)
50. S. Shoeibi, H. Kargarsharifabad, N. Rahbar, G. Ahmadi, M.R. Safaei, Performance evaluation of a solar still using hybrid nanofluid glass cooling-CFD simulation and environmental analysis. Sustain. Energy Technol. Assess. **49**, 101728 (2022)
51. E.M. Sparrow, R.D. Cess, *Radiation Heat Transfer, Augmented Edition* (1st ed. CRC Press Inc., 1978)
52. L.S. Sundar, K. Sharma, M.K. Singh, A. Sousa, Hybrid nanofluids preparation, thermal properties, heat transfer and friction factor – a review. Renew. Sustain. Energy Rev. **68**, 185–198 (2017)

53. S. Suresh, K. Venkitaraj, P. Selvakumar, M. Chandrasekar, Effect of Al2O3–Cu/water hybrid nanofluid in heat transfer. Exp. Thermal Fluid Sci. **38**, 54–60 (2012)
54. K. Swain, F. Mebarek-Oudina, S.M. Abo-Dahab, Influence of MWCNT/Fe3O4 hybrid nanoparticles on an exponentially porous shrinking sheet with chemical reaction and slip boundary conditions. J. Therm. Anal. Calorim. **147**(2), 1561–1570 (2021)
55. A. Ullah, N. Fatima, K.A.M. Alharbi, S. Elattar, I. Ikramullah, W. Khan, A numerical analysis of the hybrid nanofluid (Ag+TiO2+Water) flow in the presence of heat and radiation fluxes. Energies **16**(3), 1220 (2023)
56. A.B. Vishalakshi, U.S. Mahabaleshwar, I.E. Sarris, An MHD fluid flow over a porous stretching/shrinking sheet with slips and mass transpiration. Micromachines **13**(1), 116 (2022)
57. I. Waini, A. Ishak, I. Pop, Unsteady flow and heat transfer past a stretching/shrinking sheet in a hybrid nanofluid. Int. J. Heat Mass Transf. **136**, 288–297 (2019)
58. I. Waini, A. Ishak, I. Pop, Radiative and magnetohydrodynamic micropolar hybrid nanofluid flow over a shrinking sheet with Joule heating and viscous dissipation effects. Neural Comput. Appl. **34**(5), 3783–3794 (2021)
59. C.Y. Wang, Free convection on a vertical stretching surface. J. Appl. Math. Mech. (ZAMM) **69**, 418–420 (1989)
60. Y. Xuan, Q. Li, Investigation on convective heat transfer and flow features of nanofluids. J. Heat Transfer **125**(1), 151–155 (2003)